의학박사 학위논문

양측 와우 내 전기 자극의 위치가 양이 시간차 감도에 미치는 영향

– 백서 모델을 이용한 신경생리학적 연구 –

Effects of place of stimulation on the interaural time difference sensitivity in bilateral electrical intracochlear stimulations: Neurophysiological study in rat model

2022년 2월

서울대학교 대학원

의학과 중개의학 전공

선 우 웅 상

양측 와우 내 전기 자극의 위치가 양이 시간차 감도에 미치는 영향

– 백서 모델을 이용한 신경생리학적 연구 –

지도 교수 오 승 하

이 논문을 의학박사 학위논문으로 제출함

2021년 10월

서울대학교 대학원

의학과 중개의학 전공

선 우 웅 상

선우웅상의 의학박사 학위논문을 인준함

2022년 1월

위 원 장 _____ (인)

부위원장 _____ (인)

위　　원 _____ (인)

위　　원 _____ (인)

위　　원 _____ (인)

Abstract

Effects of place of stimulation on the interaural time difference sensitivity in bilateral electrical intracochlear stimulations: Neurophysiological study in rat model

Woongsang Sunwoo
Translational Medicine
Department of Medicine
The Graduate School
Seoul National University

With successful experience with unilateral cochlear implants (CIs) for deaf people, bilateral CIs have been used to improve hearing in noise. However, these abilities in bilateral CI users are markedly worse than that of normal-hearing listeners. This is predominantly due to the limited access of CI users to temporal information, which are created by the interaural time difference (ITD).

We examined the sensitivity of the neurons in the inferior colliculus (IC) in male and female rats to the ITDs conveyed in electrical pulse trains. Using bipolar pairs of electrodes that selectively activate the auditory nerve fibers at different intracochlear

locations, we assessed whether the responses to electrical stimulation with ITDs in different frequency regions were processed differently. Most well-isolated single units responded to the electrical stimulation in only one of the apical or basal cochlear regions, and they were classified as either apical or basal units. Regardless of the cochlear stimulating location, more than 70% of both apical and basal units were sensitive to ITDs of electrical stimulation. However, the pulse rate dependence of neural ITD sensitivity differed significantly depending on the location of the stimulation. Moreover, ITD discrimination thresholds and the relative incidence of ITD tuning type markedly differed between units activated by apical and basal stimulations. With apical stimulation, IC neurons had a higher incidence of peak-type ITD function, which mostly exhibited the steepest position of the tuning curve within the rat's physiological ITD range of ±160 μs and, accordingly, had better ITD discrimination thresholds than those with basal stimulation. These results support the idea that ITD processing in the IC might be determined by functionally segregated frequency-specific pathways from the cochlea to the auditory midbrain.

Keywords : Cochlear implant, Binaural effect, Interaural time difference, Auditory midbrain, Inferior colliculus
Student Number : 2019-34393

Table of Contents

List of Tables

List of Figure

Chapter 1. Introduction

1.1. Study Background

Cochlear implants (CIs), as advanced implantable neural stimulation devices, have become increasingly accepted as a standard treatment for profound hearing loss or deafness. Although increasing successful experience with unilateral CI over the past decades, these patients with unilateral CI frequently report having difficulty in specific conditions, such as speech understanding in noise or localization of sounds. To localize the source of sound, patients need to listen with both ears. Bilateral CIs have been used to restore binaural hearing for this purpose (Laszig et al., 2004; Neuman et al., 2007; Verschuur et al., 2005). Binaural hearing also provides advantages to speech intelligibility under noisy conditions in bilateral CI users (Laszig et al., 2004; Müller et al., 2002; Schön et al., 2002). However, the ability to locate the direction or location of a sound with bilateral CIs is still markedly worse than that of normal-hearing (NH) listeners. Previous studies demonstrated that sound localization with bilateral CIs was dominated by interaural

level differences (ILDs) while interaural time difference (ITDs) contributed only a small amount of information (van Hoesel, 2004; Seeber & Fastl, 2008).

There are several factors that restrict ITD sensitivity in bilateral CI users. Variations in sensitivity to electrically delivered ITD have been commonly found among patients. Patient-related factors of influence include the onset of deafness, periods of auditory deprivation, and the length of experience with electric hearing (Chung et al., 2019; Gordon et al., 2014; Litovsky et al., 2010; Thakkar et al., 2020). Within-patient variability in ITD sensitivity has also been observed according to parameters related to electrical stimulation, such as pulse rate, temporal modulation rate, and envelope shape (Laback et al., 2011; Noel and Eddington, 2013; van Hoesel et al., 2009). Selected CI users were able to achieve good ITD sensitivity at pulse rates up to about 100 pulses per second (pps), however ITD sensitivity of CI users typically deteriorated for higher pulse rates (Laback, Egger, & Majdak, 2015; Laback, Majdak, & Baumgartner, 2007; van Hoesel, Jones, & Litovsky, 2009). Even for stimuli under optimal conditions, only a few bilateral CI users could have the lowest ITD discrimination thresholds as low as 50 μs, roughly a factor of 4 larger than that for NH listeners (median threshold 11.5 μs) (Brughera et al., 2013;

Kan and Litovsky, 2015; Laback et al., 2015). Therefore, it can be assumed that other factors potentially affect the ITD discrimination ability.

Considering the dependence of binaural performance on frequency in acoustic hearing (Gabriel et al., 1992; Klumpp and Eady, 1956), electrode array insertion depth and cochlear frequency coverage with electrical stimulation are also thought to be possible factors influencing the performance of CI users. Low-frequency ITDs are the most dominant cues for sound localization in the horizontal plane (Wightman and Kistler, 1992). Neurons in the medial superior olive (MSO) predominantly receive low-frequency input from both ears and play an important role in processing ITDs (Guinan et al., 1972). It has been suggested that ascending pathways for encoded ITD information within the MSO, as well as within the low-frequency lateral superior olive, remain functionally segregated within the inferior colliculus (IC) (Ramachandran and May, 2002; Grothe, Pecka, & McAlpine, 2010). In addition, the presence of a high-temporal acuity brainstem pathway to the IC has been demonstrated by selective electrical stimulation of low-frequency regions of the cochlea (Middlebrooks and Snyder, 2010). Although previous clinical studies have failed to report the clear systematic effects of place of electrical stimulation on ITD

sensitivity due to individual variability, the results from best performers showed slightly better or at least similar ITD sensitivities for apical stimulation compared with the basal one (Best et al., 2011; Litovsky et al., 2010; van Hoesel et al., 2009). To improve sensitivity to ITDs in bilateral CI users, it is worth assessing whether the minimal effect of place for electrical stimulation is due to the integration of ITD information as a result of current spread or if it represents a common ITD processing mechanism for both low- and high-frequency pathways.

1.2. Hypothesis of the Study

A selective stimulation of low-frequency auditory pathways will improve ITD sensitivity in electrical hearing by a functionally segregated central processing pathway.

An alternative hypothesis is that frequency-dependent differences in acoustic ITD processing may originate from differences in cochlear processing and not from differences in central mechanisms. If the central auditory circuits specialized for binaural processing does not have a tonotopic gradient, ITD sensitivity could not vary by electrically driven inputs from the difference places of the cochlea.

1.3. Research Objectives

In the present study, we tested these hypotheses by investigating the ITD sensitivity of IC neurons to electrical stimuli presented in a bipolar configuration at different intracochlear locations.

First, we tried to control the spread of auditory neural activation more accurately by making animal bilateral CI model with a novel intracochlear electrodes' configuration. Second, we tried to assess the place effect by directly comparing the differences in neuronal ITD sensitivity between low- and high-frequency pathways by this configuration. Third, we tried to identify functionally segregated pathways by the presence of discrete physiologically defined ITD response types in the IC of this animal model.

Chapter 2. Materials and Methods

2.1. Ethical approval

All experiments were approved by the Institutional Animal Care and Use Committee at the Gachon University Gil Medical Center (approval no. MRI-2019-0007-1) and conducted at the Gachon Medical Research Institute in compliance with associated institutional guidelines and the National Institutes of Health guide for the care and use of Laboratory animals.

2.2. Animal Preparation

Experiments were conducted on 18 male and 9 female young adult (12 weeks) Wistar albino rats (448 ± 39 g and 277 ± 16 g, respectively). Rats aged 8 weeks were obtained from OrientBio Inc. (Seongnam, Korea). Rats were socially housed (two same-sex rats per cage) in conventional cages (420 x 280 x 180 mm) that were supplied with aspen bedding and nesting materials and maintained in

a temperature-controlled room (22℃, ± 2℃, 12-h light/dark cycle, and 40%-60% humidity) with ad libitum access to food and water. Cages were cleaned once a week by designated facility staff. Animals were handled only when the cage was changed to move them to a clean cage with new bedding.

Before the experiment, anesthesia was induced with a mixture of ketamine (80 mg/kg) and xylazine (10 mg/kg) administered intraperitoneally. The animals were maintained in an areflexive state for the duration of the experiment by supplemental injections of ketamine (20 mg/kg) and xylazine (3.3 mg/kg) at approximately 45-minute intervals. Appropriate anesthesia levels were tested using a toe pinch. Core body temperature was monitored with a rectal probe and maintained at >35°C using a thermostatically controlled heating pad (World Precision Instruments, Sarasota, FL, USA).

2.3. Surgical Procedures

At the beginning of the experiments, auditory brainstem responses (ABRs) to click stimuli were measured in a soundproof chamber to confirm that the animal had normal hearing (ABR threshold ≤40 dB of sound pressure level [SPL]) on both sides. For ABR recording,

TDT System 3 hardware devices (Tucker-Davis Technologies [TDT], Alachua, FL, USA) and TDT software (BioSigRP; TDT) were used. Three subdermal electrodes were inserted at the vertex and both mastoids. A 20-Hz train of click (0.1-ms) stimuli was presented in a closed field by an electrostatic speaker (EC1; TDT) coupled to a Tygon® tube with an ear tip inserted into the ear canal. Click levels varied from 80 to 5 dB SPL in 5-dB decrements. ABR data, bandpass filtered from 300 to 3000 Hz, were obtained 500 times per stimulus level and averaged. The ABR threshold was determined as the lowest level at which an identifiable waveform appeared (Fig. 1A). All 27 animals showed normal hearing thresholds on both sides, thus none of them were excluded from the present study.

Intracochlear electrodes were implanted bilaterally in the anesthetized animals. A retroauricular approach was used to open the bulla and expose the cochlea, as described previously (Mülazımoğlu et al., 2017). After the bullostomy, the stapedial artery (SA) passing between the two crura of the stapes and coursing occipitally along the promontory was visualized. The SA overlying the cochlea was cauterized and carefully removed. Lu et al. (2005) reported no significant adverse effects on the cochlear structures following cauterization of the SA. Then, two small

cochleostomies were made, one at the cochlear apex and the other at the cochlear base ventral to the round window niche to access the scala tympani of the basal turn.

For the acute deafening, to minimize hair cell-mediated responses, perilymph was aspirated, and a 10% (w/v) solution of neomycin sulfate was perfused repeatedly using a microsyringe through two cochleostomies in the basal and apical turns (Miller et al., 1998). In pilot experiments in other animals, this deafening procedure in rats consistently increased the click-evoked ABR threshold >80 dB SPL (Fig. 1B). To maintain sterile conditions, the ABRs for verifying deafness were not measured in the present experiment. After perfusion of neomycin throughout the cochlea, two additional holes were drilled into the basal and middle turns of the cochlea. These third and fourth cochleostomies went into the scala vestibuli (Fig. 2). Four stimulating electrodes, Teflon-insulated copper wires (Ø 127 μm, CU-110185; Nilaco Corp., Tokyo, Japan) with 250 μm an uncoated raw tip, were inserted separately into four drilled holes in the wall of the cochlear capsule and placed on the osseous spiral lamina close to the modiolus. The four intracochlear electrode contacts were arranged as two sets of bipolar pairs: the apical and basal electrode pairs. For each pair of electrodes, one electrode was in the scala tympani and one in the

scala vestibuli. This novel electrode configuration was expected to produce more restricted spread of excitation than is observed with the more-typical bipolar configuration used in humans and most previous animal studies in which both electrodes are in the scala tympani. After sealing the cochleostomy around the electrode with the muscle, the bulla was filled with dental cement (RelyX; ESPE, Norristown, PA, USA) to secure electrodes in place.

After intracochlear electrode placement, a midline incision was made on the scalp, and the skin flaps were retracted laterally to expose the skull. Small craniotomies were performed bilaterally rostral to lambda over the estimated position of the central nucleus of the IC (ICc), leaving the dura intact (Paxinos and Watson, 2006; Yang et al., 2018). A stainless-steel bone screw was threaded into the skull between the lambda and bregma for use as a ground electrode for recordings.

2.4. Electrical Stimulation

Immediately after the surgical procedures, the animals were placed inside a Faraday cage on an active vibration isolation table and mounted onto a stereotaxic frame (RWD Life Science, Shenzhen, China). Then, the electrode leads were connected to the electrical

stimulator. Inside the cage, a nonelectric isothermal pad was used as a source of heat to maintain the animal body temperature (Deltaphase®; Braintree Scientific, Inc., MA, USA). The animal's breathing pattern and color of extremities were checked routinely, and supplemental oxygen (1 L/min) was administered via the mask adaptor.

The RZ5P BioAmp Processor (TDT) was used with an IZV stimulator (TDT) to generate the current outputs of the signal in a bipolar electrode configuration. For bipolar stimulation, the electrode closer to the apex was assigned as the active electrode, and the other electrode was the return in each set of apical and basal electrode pairs. All configurations and controls of electrical stimulation were managed using TDT Synapse software (RRID:SCR_006495). Electric stimuli delivered to the electrodes were charge-balanced, biphasic (cathodic-leading, 40 μs per phase, with no interphase gap) pulses. The current levels were presented in 2 dB steps relative to (re) 1 mA.

To verify the appropriate function and insertion status of the implanted electrodes, electrically evoked auditory brainstem response (EABR) thresholds were measured for all four sets of bipolar electrode pairs individually in both ears (Fig. 3). A series of 40 μ s/phase biphasic current pulses were presented at a rate of 50

Hz in a bipolar stimulation mode. The EABR thresholds averaging for 400 single pulses were usually in the range of −20 to −10 dB re 1 mA.

2.5. Extracellular Single-unit Recording

The neural recording probe consisted of a single polyimide tube shank, an outside diameter of 198 μm, and a sharpened tungsten tip (Microprobes for Life Science, Gaithersburg, MD, USA). Along the shank were 4 linear platinum/iridium contact sites (diameter, 12.5 μm) centered at 150−μm intervals. Stereotaxically positioned electrodes were inserted dorsoventrally through the occipital cortex up to the IC with an oil hydraulic micromanipulator. The penetrations of the IC were verified visually after the experiments (Fig 4). Searching for single units began with the stimulation of both ears with a series of three pulses with a 100−ms interval between each pulse that was presented diotically first and then monoaurally to each ear in turn. The current levels of the search stimulus were usually set to 4 dB above the EABR thresholds. Neural signals evoked by stimulation were amplified and digitized with a PZA amplifier (TDT) and recorded with the RZ5P BioAmp Processor (TDT) at a sampling rate of 24,414 Hz. Neural activities

registered by the four electrodes were displayed online for monitoring.

Electrical artifacts were effectively reduced by the Neural Signal Referencer, the built-in function of the Synpase software that could determine common signals from a multichannel stream of neural signals and remove them. Electrical artifacts not eliminated by this method were often present, which always had a poststimulus latency <2 ms. Thus, such contaminated data were easily distinguished from neural spikes from the IC with a delay >5 ms by offline screening and were not used for data analysis.

Electrode entry into the ICc was indicated by multi-unit responses to the search stimuli. Subdivisions were solely identified electrophysiologically. The first property of the central nucleus of ICc is the presence of a tonotopic map based on seeing dorsoventral neural response changes from apical and basal stimulation. In addition, their neural properties, including low thresholds, vigorous responses, and short latencies, distinguished them from the dorsal cortex of the IC. At a depth of 1–2 mm from the surface, responses to stimulation with the apical electrode pair first appeared. This region of the IC could not be stimulated by the basal electrode pair. As the electrode was advanced ventrally, responses to the apical pair stimulation disappeared, and the basal pair stimulation

selectively elicited the neural responses from the ventral IC to a depth of 6 mm.

Single-unit spike potentials were identified by the constancy of the potential amplitude and shape. The electrode position was adjusted cautiously to improve the signal-to-noise ratio until the spikes were large enough to be reliably distinguished from background noise levels. Proper isolation of a single, discharging neuron was verified online by a principal component-based spike sorting built-in function (PCA Spike Sorting; TDT), which automatically calculated clusters based on expectation–maximization analysis of Bayesian probabilities and displayed only one cluster in the case of a well-isolated single unit. A second criterion for the clear isolation of a single unit was the interspike interval measured offline as the time between successive spontaneous spikes. If >1% of interspike intervals were <2.5 ms, the recording was considered as multi-unit activity and not used for further analysis.

2.6. Frequency Response Area Analysis

To calibrate the recording site locations in the IC, the characteristic frequencies (CFs) of the electrode sites were measured in a pilot study (1 male and 1 female rats) using a frequency response area

(FRA) analysis. Since CF cannot be measured in neurons from bilaterally deafened animals in this study, acoustic data were obtained from unilaterally implanted animals as the same method described above.

Upon isolating a single unit showing a driven response to the electrical stimulus, either apical or basal pair electrode, the monaural FRA was constructed by presenting pure tones (75−ms duration with 5−ms rise and fall times) to the contralateral normal hearing ear at a range of different frequencies (500–40,000 Hz in 25 logarithmic steps) and intensities (60–90 dB SPL in 5 dB steps). Each stimulus combination was presented five times. To determine how CFs are distributed depending on the location of intracochlear electrodes, normalized firing rates of all the FRAs were grouped according to the apical and basal stimulation and merged separately.

2.7. Data Acquisition

All single units showing responses to the search stimuli, whether excitatory or inhibitory, were included in the database and classified as either apical or basal units based on the cochlear stimulating location to which they responded. Spikes from an isolated single unit were detected and timestamped whenever a signal crossed a

voltage threshold, which was set using a fixed value depending on the shape of the spike waveform. Before investigating the responses to binaural time differences, the response threshold to the search stimuli and spontaneous firing rates (SR) during silent intervals for 30 s were measured.

Then, simultaneous binaural stimulation by pulse trains (300 ms; repetition period, 1000 ms) of the same intensity at a pulse rate of 20 pps was used to determine the first spike latency of the responses. The current levels of the stimuli were 2–4 dB above the single−pulse threshold measured using diotic search stimuli.

After responses to diotic pulse trains were recorded, ITD sensitivity was studied with binaural pulse trains that differed in relative timing in both ears. Static ITD stimuli were presented for 300 ms with a silent interval of 700 ms between successive stimuli. Initial tests were conducted at a pulse rate of 40 pps, which is an effective stimulus condition for ITD sensitivity of IC neurons (Smith and Delgutte, 2007) and at presentation levels 2–4 dB re diotic threshold. The ITDs ranged from −1500 to 1500 μs in 300 μs steps. A positive ITD value refers to a stimulus leading in the ear contralateral to the recording IC. Each ITD condition was repeated 10 times. If these current levels were not high enough to evoke responses >0.5/trial for at least one ITD, additional tests were

performed at 6–8 dB re diotic threshold. Among them, the current level displaying the best ITD sensitivity was used to investigate the influence of the pulse rate on the ITD sensitivity. For detailed measurement, ITDs were varied in steps of 200 μs from −1200 to 1200 μs, and pulse rates were varied from 20 to 1280 pps in one-octave steps. Each combination of ITD and pulse rate was tested 10 times in a pseudorandom order.

2.8. Data Analysis

A small number of units with latencies >10 ms were judged to be from the external nucleus of the IC and removed from further analysis. Thus, neural data only from the ICc were included in the study, and data from 53 apical units were compared with data from 55 basal units. Data were analyzed offline using MATLAB (The MathWorks, Inc., Natick, MA, USA, RRID:SCR_001622).

2.8.1. ITD Sensitivity Analysis

The ITD sensitivity of the recorded neuron was assessed for all the pulse rates tested by the ITD signal-to-total variance ratio (STVR) (Chung et al., 2016; Hancock et al., 2010), which was

computed as follows: after extracting the spike times, spike counts were summed over the entire 300−ms duration of the stimulus, including the first pulse in each trial. The onset response would not have varied with pulse rate because the response to the first pulse was generated prior to subsequent pulses that determined the pulse rate. Since most units had little or no sustained response at high pulse rates (≥160 pps), the computation of ITD sensitivity would have been dominated by the onset response, whereas for lower rates there would have been a larger contribution of the phase−locked sustained response (Smith and Delgutte, 2007). Based on the analysis of variance (ANOVA), ITD STVR is the ratio of the effect variance in spike counts due to changes in ITD to the total variance in spike counts across all trials. ITD STVR ranges from 0 (no ITD sensitivity), which indicates that the ITD has no effect on variance in firing rates, to 1 (perfectly reliable ITD coding), which means that the firing rates for the same ITD would be identical on every trial. To determine a statistical significance in ITD sensitivity, an F test at the $P < 0.01$ level was used. The degrees of freedom for the F test were (12, 117) when 13 ITD values were tested over 10 repetitions.

2.8.2. ITD Tuning Curve Analysis

Using the significantly ITD-sensitive response, we constructed an ITD tuning curve. The spike responses to the same ITD were averaged, and the average firing rate was plotted as a function of ITD. In each unit, the ITD tuning curves were constructed based on the responses to the pulse rate that maximize the ITD STVR.

To evaluate the shape of the ITD curve and obtain quantitative metrics of ITD sensitivity, each curve was fit with the sum of Gaussian and sigmoid functions of the following form (Chung et al., 2016):

$$\text{Rate (ITD)} = A * 2^{-\left(\frac{\text{ITD}-B}{C/2}\right)^2} + \frac{D}{1+3^{-2\left(\frac{\text{ITD}-B}{C}\right)}} + E ,$$

where B is the center of both the Gaussian and sigmoid functions, C is the half-width of the Gaussian function and the half-rise of the sigmoid function, and A, D, and E are scaling factors. The peak and trough types were classified by the presence of the central extremum, whether which was a maximum or minimum, respectively. For these two types of the fitted curve, ITDs corresponding to a local maximum or minimum of curvature were defined as the vertex ITD (ITD_{vertex}) commonly. If the firing rate decreased by >20% of the firing rate range (the difference between

maximum and minimum firing rates) for only increasing ITDs or only decreasing ITDs relative to the particular ITD showing the maximum response, the curve was classified as monotonic. The unclassified curves were poorly fit ($r^2 < 0.75$) by the template. The ITD of the maximum slope (ITD_{MS}) was obtained from the fitted curve. To avoid fitting more than one cycle within the tested ITD range of ±1200 μs, responses to pulse trains with pulse rates <320 pps were used in ITD tuning type classification.

To estimate ITD discrimination thresholds of each unit based on signal detection theory (Shackleton et al., 2003), ITD tuning curves were fitted with a cubic spline to smooth out noise. Then, a modified version of standard separation, D, was computed from the fitted curves as follows (Hancock and Delgutte, 2004):

$$D_{ITD,\ ITD+\Delta ITD} = \frac{\left|\mu_{ITD} - \mu_{ITD+\Delta ITD}\right|}{\sqrt{(\sigma^2_{ITD} + \sigma^2_{ITD+\Delta ITD})/2}},$$

where μ_{ITD} is the mean firing rate at the reference ITD, $\mu_{ITD+\Delta ITD}$ is the firing rate at the test ITD, and σ_{ITD} and $\sigma_{ITD+\Delta ITD}$ are their respective standard deviations. The just noticeable difference (JND) in ITD was defined as the lowest ΔITD at which D was ≥1. If D did not reach a value of 1 over the entire range of ITDs tested, the ITD JND was defined as unmeasurable. The reference ITD was varied from −160 to 160 μs, which approximates the rat's

physiological range for low-frequency (<3.5 kHz) ongoing ITDs (Koka et al., 2008), to optimize discrimination and find the smallest ITD JND.

2.8.3. Temporal Response Pattern Analysis

The temporal response pattern to diotic stimulation (zero ITD) was determined for each pulse rate (20-1280 pps). The temporal response pattern and average firing rate as a function of the pulse rate for a representative unit are shown in Figure. 5. In some cases, electrical stimulation produced "excitatory" responses, which resulted in increases in the average firing rate during the pulse train presentation over the background activity during the silent interval. To separate the sustained response from a burst of activity at stimulus onset and a rebound activity after stimulus, the first 50 ms post-stimulus onset as well as the first 100 ms of the silent interval were discarded. In contrast, neural activity was significantly inhibited by electrical stimulation in IC neurons with "suppressive" responses. However, in some IC neurons, both excitation and suppression patterns were elicited as the pulse rate was changed. Thus, an excitatory/suppressive (E/S) index was defined for each unit to determine the type of sustained response

based on the patterns of excitation and suppression across all pulse rates (Chung et al., 2019). The E/S index was calculated from the mean sustained firing rate curve as a function of pulse rate as follows: (E − S)/(E + S). The excitatory (E) and suppressive areas (S) are defined as the areas between two curves, specifically when the stimulus period curve is above and below, respectively, the silent period curve (Fig. 5). The E/S index is between −1 (suppressive response only) and 1 (excitatory response only).

2.9. Statistical Analysis

Sample size was selected based on preliminary electrophysiological data from 20 apical units and 23 basal units: for tests with two stimulus locations, in order to detect the significant difference of STVR, we computed a hypothetical effect size of about 0.585 in our conditions, which suggests a minimum of 47 units per group, two−tailed *t*−tests comparisons, power = 0.8 and α = 0.05. This minimum sample size was selected at the best condition producing the maximum STVR difference between two groups due to ethical considerations.

Both male and female animals were used for this study and sexes were collapsed within groups due to small sample sizes

within each group. Baseline neural properties were not significantly different between units from male and female rats (Table 1); therefore, the resulting data were pooled between sexes. Sex differences were not studied in the context of our data. We acknowledge this as a shortcoming, and all results should be interpreted with this information in mind.

Descriptive data are expressed as count (proportion, %) or mean ± standard deviation, as appropriate. "n" refers to number of neurons per group. The chi-square test was used to compare categorical variables, such as the distribution of ITD-sensitive neurons. A Fisher's exact test, a nonparametric test, was used to compare the distributions of distributions of ITD tuning types between apical and basal units. Normality of data was analyzed using the Shapiro-Wilk test. If data within a group were not normally distributed, an available transformation or a nonparametric alternative analysis was performed as specified below. To compare the fractions of ITD-sensitive neurons, as a function of pulse rate between two groups of units, two-way analysis of deviance with binomial generalized linear mixed models (GLMMs) and post hoc pairwise comparisons were run on the binary variable, which was the presence (1) or absence (0) of the ITD sensitivity at each tested pulse rate. For the effect of stimulus location, pulse rate, and

their interaction on ITD sensitivity (STVR), a two-way ANOVA with linear mixed models (LMMs) was used to test for statistical significance. ANOVAs were followed by post hoc pairwise comparison with a Bonferroni correction. The STVR, which is bounded between 0 and 1, was transformed using an arcsine transformation so that their distribution would more closely approximate the normality assumption of ANOVA. Then, a few of outliers in the basal unit group were identified using the extreme studentized deviate test, but not excluded from the analysis. Because those outliers reflect the potential high performance basal units as a normal part, removing them could make the difference from apical units more significant than it actually is. Then, a three-way ANOVA with LMMs on the arcsine transformed STVR was conducted to determine the relative contribution of onset and sustained responses on the ITD sensitivity between apical and basal units at different pulse rates. A *t* test was used to test for statistically significant differences in ITD_{MS} between apical and basal units. Shapiro-Wilk tests revealed that ITD JNDs were not normally distributed; hence, nonparametric tests (Mann-Whitney U test) were used to compare the medians of ITD JND between the apical and basal units. The criterion for significance was set at $P < 0.05$. All statistical analyses were performed in IBM SPSS Statistics

(IBM Corp., Armonk, NY, USA, RRID:SCR_019096), MATLAB (The MathWorks, Inc., Natick, MA, USA) and R 4.1.1 (R Project for Statistical Computing, Vienna, Austria, RRID:SCR_00190).

Chapter 3. Results

3.1. FRA Analysis

Apical stimulating electrodes, stimulated in bipolar configuration, selectively activated dorsally located units, corresponding to low-CF units that could not be activated by basal stimulating electrodes. In contrast, basal stimulating electrodes produced activation restricted to the ventral high-CF regions of the IC.

To calibrate the recording site locations in the IC, the CFs of the electrode sites were measured from 16 units in unilaterally implanted animals using a FRA analysis. The resulting cumulative FRA presented the lowest threshold around 2.5 kHz in the apical stimulation group (n = 6) and around 21.6 kHz in the basal stimulation group (n =10) (Fig. 6).

Based on the FRA results, the dorsally located low-CF IC units that responded to stimulation of the cochlear apex were referred to as "apical units" and that the ventrally located high-CF IC units

that responded to stimulation of the cochlear base were referred to as "basal units". We recorded the neural responses to bilateral electrical stimulation with intracochlear electrodes from 108 well-isolated single units in the ICc, of which 53 were classified as apical units and 55 as basal units.

3.2. ITD Sensitivity Analysis

It is important to note that the majority of units (77.4% of apical units and 56.9% of basal units) showed SRs <1 spike per second. Moreover, approximately 45% of the units showed no spontaneous activity. Similar proportions of units displaying no spontaneous activity were observed in the apical and basal units (50.9% and 41.2%, respectively, $\chi 2 = 0.998$ (n = 104); $P = 0.318$). Thus, the similarity in proportions of spontaneous activities between apical and basal units suggests that any difference in physiological properties related to the ITD sensitivity between the two groups of units is not likely to be caused primarily by differences in the level of anesthesia during recordings (Chung, Hancock, Nam, & Delgutte, 2014).

The dot raster (Fig. 5A) for the example apical unit shows robust short-latency (average 6.3 ms) onset responses at all pulse

rates and a sustained response phase locked to the pulse train stimulus at low pulse rates. The statistical significance of phase locking in the responses was evaluated by the Rayleigh test at the level of $P < 0.001$ (Wilkie, 1983), and phase locking of this unit was significant up to 112 pps. As the pulse rate increases, the phase-locking period tends to decrease gradually, and at pulse rates >112 pps, suppressive responses appear after a brief excitatory onset response. As can be seen from the pulse rate function in Fig. 5B, for pulse rates >320 pps, the average sustained firing rates in the interval from 50 to 300 ms after stimulus onset (red symbols) are lower than those in the silent interstimulus interval, excluding the first 100 ms (blue symbols). The E/S index values were calculated (defined in Section 2.8.3) to quantitatively evaluate the relative dominance of excitatory or suppressive responses. For example, if high SR units exhibit purely suppressive responses, the stimulus period curve will be above the silent period curve at all pulse rates such that the E/S index is a minimum of −1. Meanwhile, a maximum value of 1 represents the purely excitatory responses of the low SR units at all pulse rates. For interpretation purposes, positive and negative E/S index values were considered excitatory and suppressive response dominance, respectively. For the unit in Fig. 5B, the E/S index was 0.688, which corresponds to the relative

dominance of the excitatory response. Overall, both apical (80%) and basal (79.3%) units in the ICc showed a predominantly excitatory response. The difference between the two groups was not statistically significant (P = 0.728, Fisher's exact test). Moreover, there was no significant difference in the mean E/S index between the two groups (apical = 0.653, basal = 0.462, Mann-Whitney U test, P = 0.588).

It is The ITD sensitivity of all 108 IC units to interaurally delayed electrical pulse trains with varying stimulation rates was examined. We considered the "ITD-sensitive" units for which the ITD STVR is significantly greater than 0 at the P <0.01 level. Figure 7A shows temporal discharge patterns from an example ITD-sensitive unit as a function of ITD for a range of pulse rates (40-160 pps). The dot raster plot for 300 ms pulse trains at a rate of 40 pps shows that the neuron responds over a limited range of contralateral leading ITD (0 to +200 μs) with tightly synchronized spikes. Although 80-160 pps pulse trains also generated synchronized spikes at the favorable ITDs consistent with responses at 40 pps, responses were limited to the stimulus onset as the pulse rate increased. ITD tuning curves across all tested pulse rates are shown in Figure 7B. The mean firing rates are peaked around the contralateral-leading ITDs and obviously

modulated by ITD for all pulse rates, as indicated by the statistically significant values of the ITD STVR (Fig. 7C).

3.2.1. Fractions of ITD-Sensitive Neurons

Approximately 80% (86/108) of the units studied had a significant STVR at one or more pulse rates. The percentages of the ITD-sensitive units were not significantly different between the apical and basal units ($\chi^2(1) = 0.145$ (n = 108); $P = 0.704$) (Table 2). However, when considering the units that showed significant ITD sensitivity for at least two pulse rates, only 54.5% (30/55) of the basal units were ITD-sensitive by this criterion compared with 77.4% (41/53) of the apical units ($\chi^2(1) = 6.237$ (n = 108); $P = 0.013$). The analysis of deviance of GLMM fit for the binary ITD sensitive variable, determined by an F test at the $P < 0.01$ level from the STVR computation, revealed a statistically significant effects of both stimulus location ($\chi^2(1) = 31.536$ (n = 108); $P < 0.001$) and pulse rate ($\chi^2(6) = 52.789$ (n = 108); $P < 0.001$) on proportions of ITD-sensitive units. Post hoc analysis revealed that none of the pairwise differences reached statistically significant, except at a pulse rate of 640 pps ($z = 3.560$, $P = 0.003$ after a Bonferroni

adjustment) (Fig. 8A). For units that responded to apical stimulus, the highest proportion of ITD-sensitive units occurred at 40 pps, where 71.2% were sensitive to ITD. For basal units, the proportion of ITD-sensitive units peaked at 80 pps. As the stimulus pulse rate increased, relatively fewer neurons tended to be ITD-sensitive for both stimulus locations, and the percentages of apical units showing ITD sensitivity in the range of 320-1280 pps were still 15.5%–25% higher than those of basal units.

3.2.2. Degrees of ITD Sensitivity

The ITD STVR values, a measure of the degree of ITD sensitivity, as a function of pulse rate for apical and basal units are presented in Fig. 8B. A two-way ANOVA with LMMs on the arcsine-transformed ITD STVR was conducted to examine the effects of stimulus location and pulse rate on ITD sensitivity. The interaction effect between stimulus location and pulse rate on ITD sensitivity was statistically significant, $F_{6,\ 671.04} = 2.453$; n = 108; $P = 0.024$. Therefore, separate tests of the simple main effects for stimulus location at each pulse rate were performed. For pulse rates of 20,40, 80, and 320 pps, the arcsine transformed ITD STVR was

statistically significantly greater in apical units compared to basal units after a Bonferroni correction (n = 108; t_{680} = 4.372, P <0.001, t_{679} = 4.805, P <0.001, t_{679} = 2.992, P = 0.020, and t_{679} = 2.791, P = 0.038, respectively).

To determine the relative contribution of onset and sustained responses on the ITD sensitivity between apical and basal units at different pulse rates, a three-way ANOVA with LMMs on the arcsine transformed STVR based on two different time segments, as the first 20 ms ("onset") and the remaining 280 ms ("sustained"), was conducted.

There was no statistically significant three-way interaction between stimulus location, pulse rate, and time segment, $F_{6, 1318.8}$ = 1.880; n = 108; P = 0.081. As shown in Fig. 9., there was a statistically significant pulse rate*time segment interaction, $F_{6, 1318.8}$ = 12.180; n = 108; P < 0.001. The simple main effect of pulse rate on mean ITD STVR based on sustained responses was statistically significant $F_{6, 599.10}$ = 22.436; n = 108; P < 0.001, but not for onset responses, $F_{6, 660.18}$ = 0.595; n = 108; P = 0.734. There were statistically significant simple two-way interactions between pulse rate and time segment for both apical units, $F_{6, 625.74}$ = 13.047; n = 108; P < 0.001, and basal units, $F_{6, 648.93}$ = 4.910; n = 108; P <0.001 after a Bonferroni correction. All simple simple pairwise

comparisons were run for both apical and basal units across all pulse rates with a Bonferroni adjustment applied. In apical units, there was a statistically significant mean difference in ITD STVR between onset and sustained responses at all pulse rates except 160 and 640 pps. In contrast, basal units showed no significant differences in STVR between two separate time segments at all pulse rates (20-1280 pps).

In addition, the degree of ITD sensitivity was determined by the ability to discriminate differences in ITD using ITD JND derived from the ITD tuning curves. Fig. 10 shows the ITD JNDs as a function of the pulse rate for all 108 units. The areas of the circles at the top of the plot represent the percentage of units with undefined JNDs. Solid lines represent the median ITD JNDs, which included unmeasurable JNDs in the computations.

ITD JNDs could not be defined for more than half of the neurons at 20, 320, 640, and 1280 pps in basal units. On the other hand, only at the highest pulse rate of 1280 pps, >50% of apical units had undefined JNDs. The lowest median ITD JND occurred at 80 pps for both apical (141 μs) and basal units (612 μs). Median JNDs were significantly lower in apical units than in basal units at 20 (U = 881.5, z = −3.675, P < 0.001), 40 (U = 811.0, z = −4.055, P < 0.001), 80 (U = 907.0, z = −3.437, P = 0.001), 320 (U =

1028.5, z = −2.760, P = 0.006), and 640 pps (U = 771.0, z = −4.611, P < 0.001) (Mann-Whitney U test using an exact sampling distribution for U; with a Bonferroni correction, statistical significance was accepted at P <0.007). Remarkably, more apical units had an ITD discrimination threshold <320 μs (the maximum ITD difference, naturally possible in adult rats) than basal units across all pulse rates.

3.3. ITD Tuning Curve Analysis

When the firing rate was significantly modulated by ITD, the ITD tuning curve was constructed and fitted to define an appropriate curve type and to obtain quantitative characteristics of ITD sensitivity, including ITD_{vertex} and ITD_{MS}. The ITD functions for representative ITD−sensitive units from each ITD tuning type are presented in Fig. 11.

The ITD tuning types were determined for only a subset of the pulse rates with the highest STVR <320 pps. For clarity of exposition, we also present the temporal responses as dot raster plots with the corresponding ITD tuning curves (Fig. 11, top panels). The distributions of ITD tuning types for 42 apical and 40

basal ITD-sensitive units are presented in Table 2. Fisher's exact test showed that the multinomial probability distributions of the ITD tuning types between apical and basal stimulations were different with statistical significance (P <0.001). The majority of units that responded to the apical stimulation (28/42, 66.7%) were found to have peak-type ITD tuning curves, 14.3% were trough type, 14.3% were monotonic type, and 4.8% showed no obvious pattern. However, most basal units with ITD sensitivity displayed the monotonic type (24/40, 60%), whereas only eight basal units (20%) displayed the peak type. Trough (10%) and unclassified (10%) type curves were also observed among the basal units. Post hoc analysis involved pairwise comparisons using multiple Fisher's exact tests (2 x 2) with a Bonferroni correction. Statistical significance was accepted at P <0.0125. There were statistically significant differences in the proportion of apical units who had the peak type than basal units (P <0.001), as well as the proportion of basal units who had the monotonic type than apical units (P <0.001).

Then, parameters from the fitted ITD tuning curves were estimated to further compare ITD tuning characteristics depend on the stimulus location. ITD_{MS} was estimated from all ITD tuning curves except for the unclassified type, but ITD_{vertex} was only estimated from the peak- and trough-type curves (Fig. 11,

bottom). The distributions of ITD_{vertex} and ITD_{MS} are shown as histograms in Fig. 12.

ITD_{vertex} of the apical units showed a statistically significant contralateral bias (two-tailed t test, mean = 100 μs, t_{33} = 2.235; P = 0.032), with 73.5 % of positive ITD_{vertex} values. However, the probability distribution of ITD_{vertex} of basal units appears to be roughly different compared to apical units, although this trend marginally met statistical difference due to the relatively low incidence of peak- or trough type in the basal units (nonparametric Levene's test, P = 0.05). The ITD_{vertex} distribution for apical units was narrower (n = 34, median 150 μs, and IQR -28.8-228.5 μs) than that for basal units (n = 12, median 66.5 μs, and IQR -241.3-338.8 μs).

As shown in Fig. 12B (boxplots), Levene's test showed that the variances for the ITD_{MS} were not equal between apical and basal units, $F_{1,75}$ = 7.233; n = 77; P = 0.009. The ITD_{MS} of the apical units distributed relatively closer to the midline (zero ITD) compared with basal units; 70% of apical units, but only 43.3% of basal units, had ITD_{MS} within the physiological ITD range (χ^2_1 = 5.619 (n = 77), P = 0.018). However, there was no statistically significant difference in ITD_{MS} according to the location of stimulus (mean difference: -2.5 μs, 95% CI: -162.5-157.5 μs), $t_{54.3}$ = -

0.031; $P = 0.975$.

Chapter 4. Discussion

In psychophysical studies conducted with normal-hearing humans, ITD discrimination thresholds in sine tones was as low as 10 μs at 1000 Hz, but becoming unmeasurably high beyond 1500 Hz (Brughera, Dunai, & Hartmann, 2013; Klumpp & Eady, 1956). In the parallel pathway hypothesis, mammal sound localization uses separate binaural systems that may be involved in the processing of ITDs at low and high frequencies (Ramachandran & May, 2002). However, some authors hypothesized that the difference in ITD discrimination performance with frequency may be attributed to the sound processing characteristics in the auditory periphery as a half-wave rectifier and a low-pass filter (Colburn and Esquissaud, 1976; Van de Par and Kohlrausch, 1997). The latter assumption that a common central mechanism processes binaural temporal information across frequency has been supported by several psychophysical studies using the transposed stimuli simulating the transformation of the auditory periphery (Bernstein and Trahiotis, 2002, 2003; Van de Par and Kohlrausch, 1997). In contrast, the stimulus transposition technique suggested by van de Par and

Kohlrausch (1997) was contradicted by a neurophysiological study that demonstrated markedly different patterns in auditory nerve responses to pure and transposed tones (Dreyer and Delgutte, 2006). Thus, when acoustic stimuli are used, the binaural processing of ITDs at high and low frequencies is difficult to compare directly. Regardless of the difference in peripheral response to high- and low-frequency sounds, electrical stimulation of the auditory nerve can bypass the peripheral process and produce the same temporal discharge patterns in both low- and high-frequency auditory nerve fibers. To the best of our knowledge, no previous study has examined whether there are differences in the neural sensitivity to ITD with bilateral electrical stimulation in differing parts of the frequency map in the IC. In the present study, we compared the central binaural mechanisms underlying ITD discrimination ability at low- and high-frequency pathways by characterizing the neural ITD sensitivity to electrical pulse trains at the level of the auditory midbrain using extracellular single-unit recording methods. The major findings of the present study were the following: 1) the similarity in the overall prevalence of the ITD-sensitive units in low- and high-frequency IC regions; 2) the significant difference in the dependence of the ITD sensitivity on stimulus pulse rate according to the location of

stimulation; and 3) the different distribution of ITD tuning types between apical (low-frequency pathway) and basal (high-frequency pathway) units.

4.1. The Prevalence of the ITD-sensitive Units

Regardless of the CFs of neurons in the IC, the majority of cells (>70% of the units recorded) were sensitive to ITDs of electrical pulse trains for at least one of the tested pulse rates. Despite the multiple inputs from every brainstem auditory nucleus, there is a clear topographic representation of sound frequency in the ICc (Huang and Fex, 1986). According to its dorsoventral tonotopic organization, a low-to-high progression of the CFs as a function of depth in the ICc has been revealed (Clopton and Winfield, 1973). Accordingly, the present study showed that intracochlear bipolar electrodes at different intracochlear locations could activate the auditory system selectively and evoke cochleotopically specific activity in the IC. Thus, although the CFs of the individual IC units in the deafened animals could not be determined in this study, we considered the recorded units termed "apical" and "basal" units according to the location of an electrical stimulus as "low-CF" and "high-CF" units, respectively, corresponding to its region

activated by the stimulus.

The above neurophysiological results are in agreement with previous findings regarding the sensitivity to ITDs of sound stimulation in the rat's ICc (Kidd and Kelly, 1996). Since most neurons in the rat's ICc have CFs >1 kHz (Kelly et al., 1991; Zhang and Kelly, 2010), it is not possible to evaluate the dependence on the CF of the ITD sensitivity to tone stimuli at such high frequencies. Using transient stimuli (clicks), it is possible to create dichotic stimuli that have an onset time difference. Previously, ITD sensitivity in response to clicks has been demonstrated for neurons in the auditory cortex of rats (Kelly and Phillips, 1991). Subsequently, Kidd and Kelly (1996) also showed that virtually every tested neuron in the ICc of the rat was sensitive to ITDs of clicks when it generated an contralateral excitatory-ipsilateral inhibitory (EI) binaural response patterns to tone bursts at CF, regardless of the CF. Zhang and Kelly (2010) reported that the majority (67%) of neurons in the rat's ICc displayed an EI binaural interaction, which may explain the similar proportion of ITD-sensitive neurons in the IC compared with our results. Moreover, experiments with low-CF IC neurons (<3 kHz) in the cat showed similarities between the sensitivities to ITDs of clicks and wideband noise (0-4 kHz); in particular, the click responses

resembled the transient-onset response to the noise stimulus (Carney and Yin, 1989). Therefore, it is apparent that most IC neurons across the CF range have ITD sensitivity, at least based on the onset responses to sound stimulation. In the present study, to analyze ITD sensitivity, we also included the onset responses of IC neurons to electrical pulse trains, because the relative contributions of onset and sustained responses vary with pulse rate (Smith and Delgutte, 2007). Previous studies in bilaterally implanted cats by Smith and Delgutte (2007) showed that the inclusion of onset responses improved neural ITD JNDs in IC neurons as the pulse rate increased. Even when the electrical pulse trains were presented at 160 and 320 pps, the ITD discrimination thresholds were dominated by the onset responses.

4.2. The Pulse Rate Dependence of Neural ITD Sensitivity

Generally, it has been shown that the ITD sensitivity of IC neurons to electrical stimulation is best at low pulse rates <100 pps and progressively worsens with increasing pulse rate (Chung et al., 2016; Smith and Delgutte, 2007). Consistent with previous studies, our results showed that changing pulse rates had a similar demonstrable effect on both the fraction of ITD-sensitive neurons

and the degree of ITD sensitivity in the IC (Figs. 4 and 8). As one of the main goals of this study, we are particularly interested in whether the dependence of neural ITD sensitivity on pulse rate is influenced by the stimulus location. The results based on the ITD STVR analysis showed a wider range of pulse rates over which neurons were sensitive to ITD in apical units than in basal units. Significant ITD sensitivity to pulse rates up to 320 pps was observed in more than half of the apical units, and 37.7% of apical units were still sensitive to ITD even at a pulse rate of 1280 pps. However, for the basal units, the prevalence of ITD-sensitive units peaked at pulse rates of 80 pps, and >50% were ITD-sensitive only at 40-80 pps. Comparison of STVR based on the onset response with those based on the and sustained response indicated that, ITD sensitivity in apical units was dominated by the sustained response up to 80 pps and dominated by the onset response at 320, 640, and 1280 pps, whereas ITD sensitivity in basal units was not dominated by the sustained response even at 20 pps, the lowest pulse rates tested. Moreover, neural ITD JNDs obtained with apical stimulation were consistently smaller than those obtained with basal stimulation at low pulse rates (<100 pps). More than half of the units showed unmeasurable ITD JNDs to basal stimulation, with pulse rates >320 pps. In response to apical stimulation, the median JND could not be

determined at 1280 pps. Collectively, our findings indicate that the pulse rate-dependent degradation in neural ITD sensitivity at higher pulse rates is more severe in basal units than in apical units.

Middlebrooks and Snyder (2010) explored phase-locked responses of neurons in the cat's IC to monoaural electrical pulse trains with intraneural electrodes, which could activate frequency-specific regions of the IC. They measured the highest pulse rates for significant phase locking (limiting rates) and first-spike latencies as functions of the CFs of the IC units. Most IC units with high CFs (>1.5 kHz) tended to have lower pulse-locking limits (<400 pps), defined as the highest pulse rate where synchronization was observed between neural spikes and stimulus pulses, than low-CF (<1.5 kHz) IC units. In addition, units with higher pulse-locking limits (>300 pps) tended to have shorter first-spike latencies (<6 ms) (Middlebrooks and Snyder, 2010). These results demonstrated the presence of a low-frequency brainstem pathway specialized for preservation of temporal fine structure, which supports our hypothesis that binaural temporal processing in the IC might be determined by functionally segregated pathways that are associated with the stimulation of different tonotopic places in the cochlea.

4.3. The Incidence of ITD Tuning Types

A novel finding of this study was that the relative incidence of ITD tuning types markedly differed between the apical (low-CF) and basal (high-CF) units. Of the 42 ITD-sensitive units for apical stimulation, the most common ITD classification was peak type (66.7%). However, the monotonic type (24/40, 60%) was most commonly observed for basal units with ITD sensitivity. The distributions of the ITD tuning type reported in this study are consistent with those of previous studies of single-unit responses in the IC (Haqqee et al., 2021; McAlpine et al., 2001). The majority of low-CF units (< 1.5 kHz) showed peaks at the contralaterally leading ITDs of noise bursts (50 Hz-5 kHz) and were classified as peak type in the IC of the guinea pig (McAlpine et al., 2001). In addition, similar proportions of high-CF units in the IC of the bat largely displayed monotonic ITD sensitivity to high-frequency tones (20-50 kHz), with a minority showing trough and peak types (Haqqee et al., 2021).

Interestingly, significant effect of stimulus location on the distribution of ITD tuning metrics derived from the fitted curves, especially on the ITD_{MS}, was found. As shown in figure 6, the distributions of ITD_{MS} among IC neurons depended on the type of

ITD tuning curve. Of the 36 peak-type ITD-sensitive units, 27 (75%) exhibited the steepest positions of the unit's tuning curve (ITD_{MS}) within the rat's behaviorally relevant ITD range of ±160 μs. Conversely, 20 (66.6%) of 30 monotonic-type ITD-sensitive units were most sensitive to ITDs outside the behaviorally relevant ITD range. Based on the coding strategy at the single-neuron level, ITD discrimination is the most sensitive along the maximum slope of the neuron's tuning curve. Thus, the dominance of the peak-type in apical units could be one of the possible explanations for their higher ability to discriminate ITDs (ITD JNDs) compared with basal units with monotonic-type dominance. Similarly, previous studies of IC in neonatally deafened rabbits reported an increased incidence of monotonic-type units, fewer peak-type units, and poorer ITD JNDs compared with acutely deafened animals (Chung et al., 2019). Despite better discrimination ability to ITDs of electrical stimulation at the cochlear apex than at the cochlear base, it is difficult to assert that rats would better utilize such cues delivered from the apex for sound localization based solely on neurophysiological data. To confirm the effects of stimulus location on behavioral sensitivity in rats, psychoacoustic studies on sensitivity to ITDs of electrical stimulation delivered in the same way as this study are required.

In a previous study, Chung et al. (2016) reported that the distribution of ITD tuning type varied with pulse rate. For low pulse rates (20-40 pps), the monotonic type was the most common. As pulse rates increase, the peak type becomes the most common type at 80-160 pps (Chung et al., 2016). In the present study, the pulse rates showing the highest STVR were selected to fit the ITD tuning curves, and the pulse rates reported in both apical and basal units were approximately evenly distributed between 20 and 160 pps. Because their distributions were similar, we suggest that the relationship between the cochleotopic region and the predominant type of ITD tuning observed in the IC might reflect properties of brainstem pathways and support the concept of parallel processing pathways proposed by Ramachandran and May (2002).

The central auditory system is comprised of a complex network of specialized synaptic connections that coordinate the flow of information through it. Identifying connections between neuronal populations using neural tracing techniques could provide the strong evidence directly and support the concept of parallel processing pathways in electrical hearing. To test whether inputs from functionally different brainstem sources are segregated or converge on the same neurons in the ICc, anterograde labeling of axons from the superior olivary complex (SOC) and retrograde transport

experiments in the ICc have been performed (Oliver et al., 1997; Loftus et al., 2004). These data suggested that the pattern of projections from the SOC changed in the transition from lower frequency to higher frequency ICc. Consequently, separate domains of postsynaptic neurons for low-frequency and high-frequency inputs could maintain a separation of type of binaural responses in the ICc.

Based on similar correspondence in frequency-response map features and the binaural properties of the single-unit responses in the auditory brainstem, the differential representation of temporal processing in the ICc has been demonstrated to derive from their respective sources at the lower brainstem level (Ramachandran and May, 2002). The contribution of the MSO, which has been characterized as a predominantly low-frequency nucleus (Guinan et al., 1972), is apparent from the tendency of MSO units to show peak-type ITD responses (Batra et al., 1997). Peak-type responses are associated with the coincidence of binaural excitatory inputs in the MSO, whereas monotonic-type ITD responses are thought to reflect binaural suppression from the lateral superior olive or dorsal nucleus of the lateral lemniscus. In accordance with this latter assumption, such EI neurons in the rat IC typically have a monotonic ITD function for click stimuli (Kidd

and Kelly, 1996). In addition, Kelly et al. (1991) demonstrated a tendency for EI response patterns to be more common in high-CF (>4 kHz) IC neurons in rats. For monotonic-type neurons, neural ITD processing can be affected by the interaural intensity difference (Irvine et al., 1995). Lowering the intensity of ipsilateral stimulation reduced the strength and duration of the inhibitory effect, and vice versa. Consequently, simultaneous ILD changes during free-field sound localization would cause ITD tuning of monotonic-type neurons to shift outside the behaviorally relevant range. Therefore, although both peak- and monotonic-type IC neurons are sensitive to ITDs of electrical stimulation, selective apical stimulation of the low-frequency pathway could lead to better sensitivity to ITDs compared with basal stimulation.

4.4. Limitations of the Study

Among the currently available electrode designs, the FLEX SOFT electrode (MED-EL, Austria) with an array length of 31.5 mm is the longest electrode and has the maximum insertion depth (nearly into the end of the middle turn of the cochlea). Recently, Ausili et al. (2020) tested 25 bilateral CI recipients implanted with the FLEX SOFT or STANDARD electrode array with fine-structure temporal

processing as encoding strategy in the low-frequency channels (up to 1 kHz). Using this encoding strategy in the low-frequency channels, the temporal representation of the low-frequency fine structure can be potentially improved. Results showed that none of subjects with fine-structure coding had ITD perception within the physiological range, although there was a large variability in performance. Unfortunately, for the MED-EL manufacture, the device can be programmed in a monopolar stimulation mode only. As a result, psychophysical data on the sensitivity of users of deeply inserted long electrodes to ITDs of similar selective electrical stimulation in bipolar configurations are lacking. Thus, the effect of selective apical and basal stimulations on ITD discrimination ability in electric hearing remains to be tested.

Second, the bipolar pairs available in humans, with both electrodes in the scala tympani, probably do not achieve the selective stimulation that was achieved in the present study, in which the bipolar pair comprised scala tympani and scala vestibuli electrodes. To simulate a clinically applicable situations, the further experiments with a two-channel intracochlear electrode array would be required. In addition, such pair of electrodes which are visually positioned independently could lead to an interaural pair eliciting the different place pitch in the two ears. Even if there was

a possible place mismatching, which can be considered to be minimal because only the binaural IC neurons showing robust responses bilaterally were included in this study.

Third, we test the hypothesis that the degradation in ITD processing with bilateral CI is due to inability to use central pathways specialized for ITD processing rather than limitations in peripheral encoding in the acutely deafened adult animal model. Thus, our results are only relevant to adult cases of acute deafness of relatively short duration to minimize developmental abnormalities and degenerative changes in the binaural pathways resulting from prolonged deafness like prelingual deafness cases. Snyder et al. (1990) indicated that the orderly topographic representation of the central auditory organization is unaltered by the lack of normal acoustic input during development at least to the level of the midbrain. However, such development of cochleotopic representation in the central auditory pathway in the neonatally deafened animal does not mean functionally segregated pathway related to binaural processing. Therefore, further studies to test our hypothesis in the neonatally deafened animal model are required.

4.5. Clinical Implications

This section discusses how this improved understanding of effects of spatial selectivity can help account for the psychophysical results and develop new clinical devices. The present findings are in contrast with psychophysical studies conducted with human CI listeners. If the responses reflect the broad electrical field with monopolar stimulation, selective stimulation will likely produce improvement in the performance of ITD detection. In this regard, our results lay the groundwork for investigating whether the degradations in ITD sensitivity observed in acutely deafened adult animals can be improved by appropriate CI stimulation of low-frequency specific pathway.

In the ITD processing of more complex stimuli such as speech and language with CIs, a more selective stimulation of apical fibers would be required because multiple interaural electrode pairs are stimulated. Patra et al. (2011) et al. suggested that high-frequency noise bands at high levels could generate significant low-frequency masking in normal-hearing listeners. It also seems to hold in CI users, particularly in case of a large current spread to apical fibers from more basal electrodes, nonsynchronized activity in high-frequency pathways stimulated at higher levels might mask perception of ITDs through low-frequency pathways that might have some implications for sound localization and speech perception

in noise. Therefore, we suggest that the development of a clinically practicable auditory prosthesis for more selective stimulation of low-frequency pathways would be required to enhance sensitivity to ITDs.

Chapter 5. Conclusions

In summary, we found that, compared with stimulation at the basal turn of the cochlea, presenting ITDs of electrical pulse trains at an apical electrode pair resulted in improved ITD sensitivity when the dependence of pulse rates was considered. The results suggest that differences in ITD discrimination thresholds between apical (low-CF) and basal (high-CF) IC units are primarily due to the relative proportions of the ITD tuning types rather than the intrinsic properties for electrical stimulation. These findings support the idea that ITD processing in the IC might be determined by functionally segregated frequency-specific pathways from the cochlea to the auditory midbrain.

Bibliography

1. Ausili, S. A., Agterberg, M. J. H., Engel, A., Voelter, C., Thomas, J. P., Brill, S., Snik, A. F. M., Dazert, S., Van Opstal, A.J., Mylanus, E. A. M. (2020). Spatial Hearing by Bilateral Cochlear Implant Users With Temporal Fine-Structure Processing. Front Neurol, 11, 915. doi:10.3389/fneur.2020.00915.
2. Batra, R., Kuwada, S., and Fitzpatrick, D.C., (1997). Sensitivity to interaural temporal disparities of low- and high-frequency neurons in the superior olivary complex. I. Heterogeneity of responses. J Neurophysiol 78(3), 1222-1236.
3. Bernstein, L.R., and Trahiotis, C., (2002). Enhancing sensitivity to interaural delays at high frequencies by using "transposed stimuli". J Acoust Soc Am 112(3), 1026-1036.
4. Bernstein, L.R., and Trahiotis, C., (2003). Enhancing interaural-delay-based extents of laterality at high frequencies by using "transposed stimuli". J Acoust Soc Am 113(6), 3335-3347.
5. Best, V., Laback, B., and Majdak, P., (2011). Binaural interference in bilateral cochlear-implant listeners. J Acoust Soc Am 130(5), 2939-2950.

6. Brughera, A., Dunai, L., and Hartmann, W.M., (2013). Human interaural time difference thresholds for sine tones: the high-frequency limit. J Acoust Soc Am 133(5), 2839-2855.
7. Carney, L.H., and Yin, T.C., (1989). Responses of low-frequency cells in the inferior colliculus to interaural time differences of clicks: excitatory and inhibitory components. J Neurophysiol 62(1), 144-161.
8. Chung, Y., Buechel, B.D., Sunwoo, W., Wagner, J.D., and Delgutte, B., (2019). Neural ITD Sensitivity and Temporal Coding with Cochlear Implants in an Animal Model of Early-Onset Deafness. J Assoc Res Otolaryngol 20(1), 37-56.
9. Chung, Y., Hancock, K.E., and Delgutte, B., (2016). Neural Coding of Interaural Time Differences with Bilateral Cochlear Implants in Unanesthetized Rabbits. J Neurosci 36(20), 5520-5531.
10. Chung, Y., Hancock, K. E., Nam, S. I., & Delgutte, B. (2014). Coding of electric pulse trains presented through cochlear implants in the auditory midbrain of awake rabbit: comparison with anesthetized preparations. J Neurosci, 34(1), 218-231.
11. Clopton, B.M., and Winfield, J.A., (1973). Tonotopic organization in the inferior colliculus of the rat. Brain Res 56, 355-358.

12. Colburn, H.S., and Esquissaud, P., (1976). An auditory-nerve model for interaural time discrimination of high-frequency complex stimuli. J Acoust Soc Am 59(S1), S23-S23.
13. Dreyer, A., and Delgutte, B., (2006). Phase locking of auditory-nerve fibers to the envelopes of high-frequency sounds: implications for sound localization. J Neurophysiol 96(5), 2327-2341.
14. Gabriel, K.J., Koehnke, J., and Colburn, H.S., (1992). Frequency dependence of binaural performance in listeners with impaired binaural hearing. J Acoust Soc Am 91(1), 336-347.
15. Gordon, K.A., Deighton, M.R., Abbasalipour, P., and Papsin, B.C., (2014). Perception of binaural cues develops in children who are deaf through bilateral cochlear implantation. PLoS One 9(12), e114841.
16. Grothe, B., Pecka, M., & McAlpine, D. (2010). Mechanisms of sound localization in mammals. Physiol Rev, 90(3), 983-1012.
17. Guinan, J.J., Norris, B.E., and Guinan, S.S., (1972). Single Auditory Units in the Superior Olivary Complex: II: Locations of Unit Categories and Tonotopic Organization. International Journal of Neuroscience 4(4), 147-166.
18. Hancock, K.E., and Delgutte, B., (2004). A physiologically based model of interaural time difference discrimination. J Neurosci

24(32), 7110-7117.

19. Hancock, K.E., Noel, V., Ryugo, D.K., and Delgutte, B., (2010). Neural coding of interaural time differences with bilateral cochlear implants: effects of congenital deafness. J Neurosci 30(42), 14068-14079.
20. Haqqee, Z., Valdizón-Rodríguez, R., and Faure, P.A., (2021). High frequency sensitivity to interaural onset time differences in the bat inferior colliculus. Hear Res 400, 108133.
21. Huang, C.M., and Fex, J., (1986). Tonotopic organization in the inferior colliculus of the rat demonstrated with the 2-deoxyglucose method. Exp Brain Res 61(3), 506-512.
22. Irvine, D.R., Park, V.N., and Mattingley, J.B., (1995). Responses of neurons in the inferior colliculus of the rat to interaural time and intensity differences in transient stimuli: Implications for the latency hypotheses. Hear Res 85(1-2), 127-141.
23. Kan, A., and Litovsky, R.Y., (2015). Binaural hearing with electrical stimulation. Hear Res 322, 127-137.
24. Kelly, J.B., Glenn, S.L., and Beaver, C.J., (1991). Sound frequency and binaural response properties of single neurons in rat inferior colliculus. Hear Res 56(1-2), 273-280.
25. Kelly, J.B., and Phillips, D.P., (1991). Coding of interaural time differences of transients in auditory cortex of Rattus

norvegicus: implications for the evolution of mammalian sound localization. Hear Res 55(1), 39-44.

26. Kidd, S.A., and Kelly, J.B., (1996). Contribution of the dorsal nucleus of the lateral lemniscus to binaural responses in the inferior colliculus of the rat: interaural time delays. J Neurosci 16(22), 7390-7397.
27. Klumpp, R.G., and Eady, H.R., (1956). Some Measurements of Interaural Time Difference Thresholds. J Acoust Soc Am 28(5), 859-860.
28. Koka, K., Read, H.L., and Tollin, D.J., (2008). The acoustical cues to sound location in the rat: measurements of directional transfer functions. J Acoust Soc Am 123(6), 4297-4309.
29. Kral, A., Hartmann, R., Mortazavi, D., and Klinke, R., (1998). Spatial resolution of cochlear implants: the electrical field and excitation of auditory afferents. Hear Res 121(1-2), 11-28.
30. Laback, B., Majdak, P., & Baumgartner, W. D. (2007). Lateralization discrimination of interaural time delays in four-pulse sequences in electric and acoustic hearing. J Acoust Soc Am, 121(4), 2182-2191.
31. Laback, B., Egger, K., and Majdak, P., (2015). Perception and coding of interaural time differences with bilateral cochlear implants. Hear Res 322, 138-150.

32. Laback, B., Zimmermann, I., Majdak, P., Baumgartner, W.D., and Pok, S.M., (2011). Effects of envelope shape on interaural envelope delay sensitivity in acoustic and electric hearing. J Acoust Soc Am 130(3), 1515-1529.

33. Laszig, R., Aschendorff, A., Stecker, M., Müller-Deile, J., Maune, S., Dillier, N., Weber, B., Hey, M., Begall, K., Lenarz, T., et al., (2004). Benefits of bilateral electrical stimulation with the nucleus cochlear implant in adults: 6-month postoperative results. Otol Neurotol 25(6), 958-968.

34. Litovsky, R.Y., Jones, G.L., Agrawal, S., and van Hoesel, R., (2010). Effect of age at onset of deafness on binaural sensitivity in electric hearing in humans. J Acoust Soc Am 127(1), 400-414.

35. Loftus, W. C., Bishop, D. C., Saint Marie, R. L., & Oliver, D. L. (2004). Organization of binaural excitatory and inhibitory inputs to the inferior colliculus from the superior olive. J Comp Neurol, 472(3), 330-344.

36. Lu, W., Xu, J., and Shepherd, R.K., (2005). Cochlear implantation in rats: a new surgical approach. Hear Res 205(1-2), 115-122.

37. McAlpine, D., Jiang, D., and Palmer, A.R., (2001). A neural code for low-frequency sound localization in mammals. Nat Neurosci

4(4), 396-401.

38. Middlebrooks, J.C., and Snyder, R.L., (2010). Selective electrical stimulation of the auditory nerve activates a pathway specialized for high temporal acuity. J Neurosci 30(5), 1937-1946.

39. Miller, C.A., Abbas, P.J., Rubinstein, J.T., Robinson, B.K., Matsuoka, A.J., and Woodworth, G., (1998). Electrically evoked compound action potentials of guinea pig and cat: responses to monopolar, monophasic stimulation. Hear Res 119(1-2), 142-154.

40. Mülazımoğlu, S., Ocak, E., Kaygusuz, G., and Gökcan, M.K., (2017). Retroauricular Approach for Targeted Cochlear Therapy Experiments in Wistar Albino Rats. Balkan Med J 34(3), 200-205.

41. Müller, J., Schön, F., and Helms, J., (2002). Speech understanding in quiet and noise in bilateral users of the MED-EL COMBI 40/40+ cochlear implant system. Ear Hear 23(3), 198-206.

42. Neuman, A.C., Haravon, A., Sislian, N., and Waltzman, S.B., (2007). Sound-direction identification with bilateral cochlear implants. Ear Hear 28(1), 73-82.

43. Noel, V.A., and Eddington, D.K., (2013). Sensitivity of bilateral

cochlear implant users to fine-structure and envelope interaural time differences. J Acoust Soc Am 133(4), 2314-2328.

44. Oliver, D. L., Beckius, G. E., Bishop, D. C., & Kuwada, S. (1997). Simultaneous anterograde labeling of axonal layers from lateral superior olive and dorsal cochlear nucleus in the inferior colliculus of cat. J Comp Neurol, 382(2), 215-229.

45. Patra, H., Roup, C. M., & Feth, L. L. (2011). Masking of low-frequency signals by high-frequency, high-level narrow bands of noise. J Acoust Soc Am, 129(2), 876-887. doi:10.1121/1.3518778.

46. Paxinos, G., and Watson, C., (2006). The rat brain in stereotaxic coordinates, 6th ed. Academic Press, San Diego, CA.

47. Ramachandran, R., and May, B.J., (2002). Functional segregation of ITD sensitivity in the inferior colliculus of decerebrate cats. J Neurophysiol 88(5), 2251-2261.

48. Schön, F., Müller, J., and Helms, J., (2002). Speech reception thresholds obtained in a symmetrical four-loudspeaker arrangement from bilateral users of MED-EL cochlear implants. Otol Neurotol 23(5), 710-714.

49. Seeber, B. U., & Fastl, H. (2008). Localization cues with bilateral cochlear implants. J Acoust Soc Am, 123(2), 1030-

1042.

50. Shackleton, T.M., Skottun, B.C., Arnott, R.H., and Palmer, A.R., (2003). Interaural time difference discrimination thresholds for single neurons in the inferior colliculus of Guinea pigs. J Neurosci 23(2), 716-724.

51. Smith, Z.M., and Delgutte, B., (2007). Sensitivity to interaural time differences in the inferior colliculus with bilateral cochlear implants. J Neurosci 27(25), 6740-6750.

52. Snyder R.L., Rebscher S.J., Cao K.L., Leake P.A., and Kelly K., (1990). Chronic intracochlear electrical stimulation in the neonatally deafened cat. I: Expansion of central representation. Hear Res 50(1-2), 7-33.

53. Snyder, R.L., Bierer, J.A., and Middlebrooks, J.C., (2004). Topographic spread of inferior colliculus activation in response to acoustic and intracochlear electric stimulation. J Assoc Res Otolaryngol 5(3), 305-322.

54. Sunwoo, W., and Oh, S.H., (2021). Effects of place of stimulation on the interaural time difference sensitivity in bilateral electrical intracochlear stimulations: Neurophysiological study in a rat model. J Neurosci Res. doi: 10.1002/jnr.24991. Epub ahead of print.

55. Thakkar, T., Anderson, S.R., Kan, A., and Litovsky, R.Y.,

(2020). Evaluating the Impact of Age, Acoustic Exposure, and Electrical Stimulation on Binaural Sensitivity in Adult Bilateral Cochlear Implant Patients. Brain Sci 10(6).

56. van de Par, S., and Kohlrausch, A., (1997). A new approach to comparing binaural masking level differences at low and high frequencies. The Journal of the Acoustical Society of America 101(3), 1671-1680.
57. van Hoesel, R. J. (2004). Exploring the benefits of bilateral cochlear implants. Audiol Neurootol, 9(4), 234-246.
58. van Hoesel, R.J., Jones, G.L., and Litovsky, R.Y., (2009). Interaural time-delay sensitivity in bilateral cochlear implant users: effects of pulse rate, modulation rate, and place of stimulation. J Assoc Res Otolaryngol 10(4), 557-567.
59. Verschuur, C.A., Lutman, M.E., Ramsden, R., Greenham, P., and O'Driscoll, M., (2005). Auditory localization abilities in bilateral cochlear implant recipients. Otol Neurotol 26(5), 965-971.
60. Wightman, F.L., and Kistler, D.J., (1992). The dominant role of low-frequency interaural time differences in sound localization. J Acoust Soc Am 91(3), 1648-1661.
61. Wilkie, D., 1983. Rayleigh Test for Randomness of Circular Data. Journal of the Royal Statistical Society. Series C (Applied Statistics) 32(3), 311-312.

62. Yang, P., Wang, Z., Zhang, Z., Liu, D., Manolios, E.N., Chen, C., Yan, X., Zuo, W., and Chen, N., (2018). The extended application of The Rat Brain in Stereotaxic Coordinates in rats of various body weight. J Neurosci Methods 307, 60-69.
63. Zhang, H., and Kelly, J.B., (2009). Time-dependent effects of ipsilateral stimulation on contralaterally elicited responses in the rat's central nucleus of the inferior colliculus. Brain Res 1303, 48-60.
64. Zhang, H., and Kelly, J.B., (2010). Time dependence of binaural responses in the rat's central nucleus of the inferior colliculus. Hear Res 268(1-2), 271-280.

Table 1. Sex Differences as a Biological Variable.

	Male (n = 47)	Female (n = 61)	
Apical vs Basal units	22:25	31:30	$\chi^2(1) = 0.171$ $P = 0.679$ †
Number of ITD-sensitive units (%)	34 (72.3%)	52 (85.2%)	$\chi^2(1) = 2.726$ $P = 0.099$ †
First spike latency (ms)	7.06 ± 2.73	7.48 ± 1.90	$t_{56.466} = -0.795$ $P = 0.430$ ‡
Number of unsynchronized units (%)	8/38 (21.1%)	7/50 (14.0%)	$\chi^2(1) = 0.759$ $P = 0.383$ †

† $\chi 2$ test

‡ *t* test

Table 2. Distribution of ITD Tuning Types.

	ITD−insensitive units	ITD−sensitive units (n = 82)†			
		Peak	Trough	Monotonic	Unclassified
Apical units	18.9% (10/53)	28 (66.7%)	6 (14.3%)	6 (14.3%)	2 (4.8%)
Basal units	21.8% (12/55)	8 (20.0%)	4 (10.0%)	24 (60.0%)	4 (10.0%)
	χ^2_1 = 0.145 (n = 108) P = 0.704‡	P <0.001§	p = 0.738§	p <0.001§	P = 0.427§

†Analysis limited to units with ITD sensitivity for at least one pulse rate below 320 pps

‡χ^2 test

§Fisher's exact tests (2 x 2) with a Bonferroni correction, statistical significance accepted at P <0.0125.

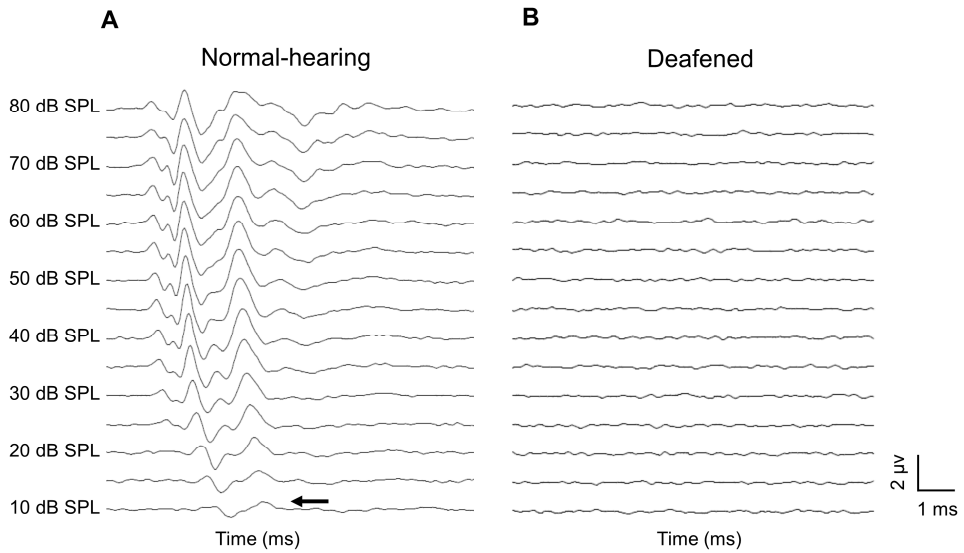

Figure 1. Example auditory brainstem responses (ABRs) from (A) normal-hearing and (B) acutely deafened rats. ABRs are plotted stacked for increasing stimulus level, from 10 to 80 dB sound pressure level (SPL). Responses were evoked by clicks. (A) Typical ABR obtained from a normal-hearing animal is shown. The threshold is indicated by an arow. (B) Recordings from an acutely deafened rat where no visible responses were measured up to 80 dB SPL is shown.

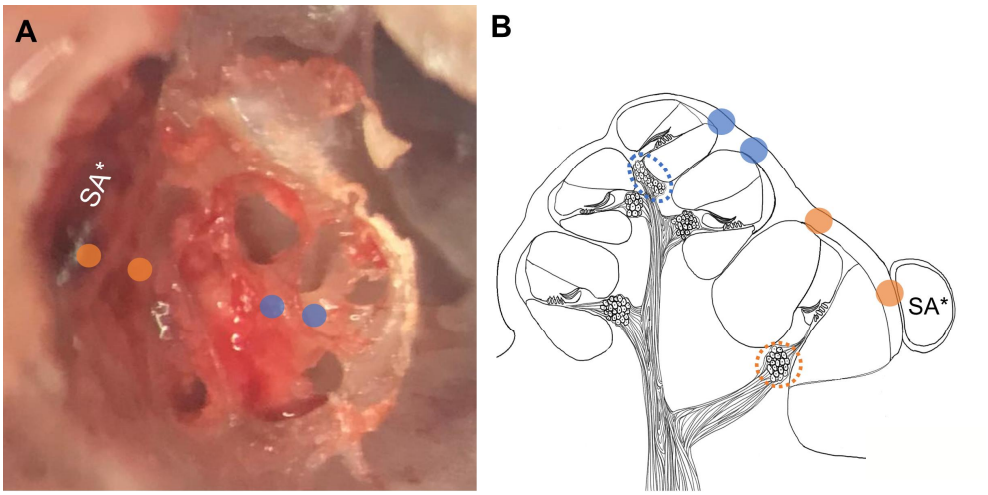

Figure 2. Four cochleostomy positions for implanting two sets of bipolar electrodes. (A) The lateral bony cochlear wall is removed to expose the modiolus. Color-filled circles indicate the ideal cochleostomy sites to reach the expected target area. (B) Schematic drawing in a perimodiolar cross section of rat cochlea. The target spiral ganglions within the Rosenthal canal are indicated by dotted circles for apical (blue) and basal (orange) electrodes pairs. *The stapedial artery (SA) overlying the cochlea will be cauterized.

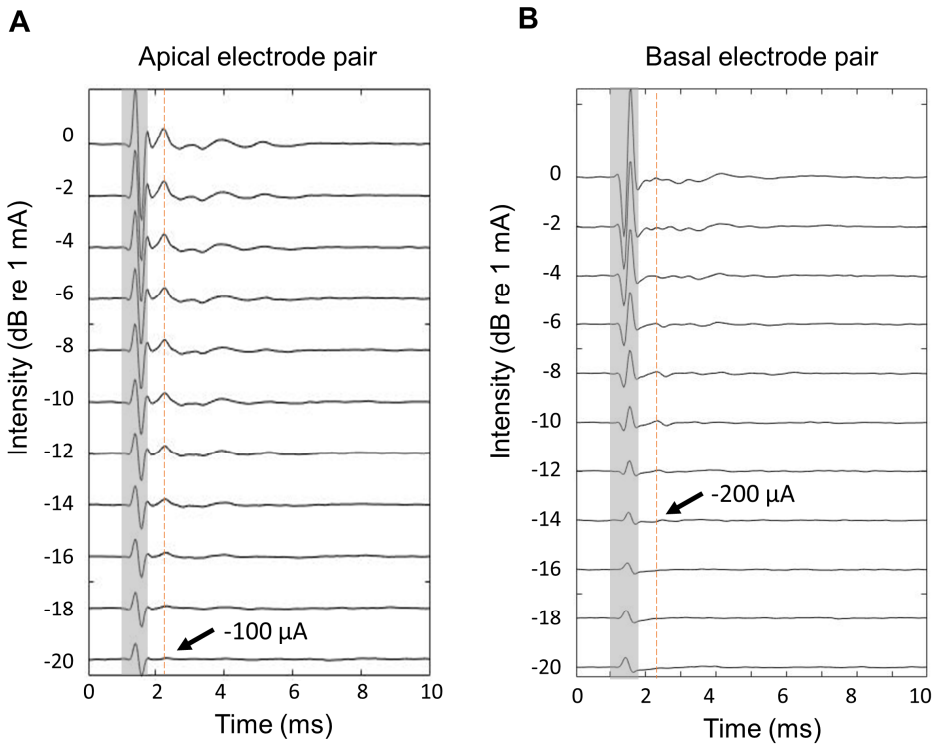

Figure 3. Example electrically evoked auditory brainstem responses (EABRs) to the (A) apical and (B) basal electrode pair stimulation in acutely deafened rats. A biphasic pulse train is presented in bipolar configuration at 50 pulses per second with 400 repetitions. Stimuli level from 100 μA to 1 mA is shown in 2 dB steps. Arrows and numerals denote EABR thresholds. The wave latencies (vertical dotted line) are not changed with increasing current level. Gray area indicates the electrical stimulation coherent artifacts.

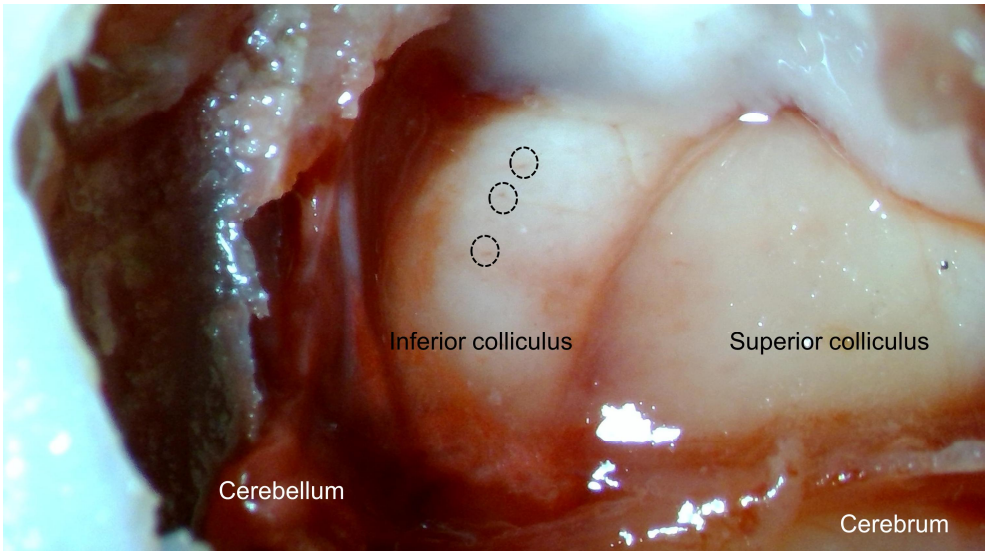

Figure 4. Verification of penetrating into the inferior colliculus (IC). Dissection picture of the brain showing three tracks of recording electrode (the dotted circles) on the right IC. The structures of the brain are indicated.

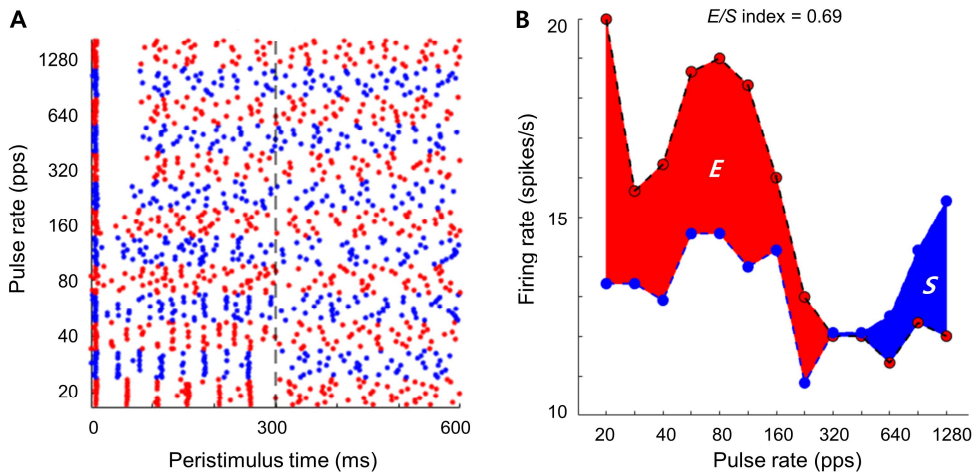

Figure 5. Temporal response patterns (A) and average sustained firing rates (B) to electrical pulse trains of varying pulse rates for an example neuron in the inferior colliculus. (A) In a dot raster plot, alternating color rows display blocks of trials at different pulse rates. (B) Red– and blue–filled circles indicate average spike times occurring 50–300 and 400–600 ms after stimulus onset, respectively. The area between the two curves indicates either the amount of excitatory response (E area) or suppressive response (S area) relative to the spontaneous activities. The positive value of the ES index (defined in Section 2.8.3) in this unit represents the relative dominance of excitatory responses.

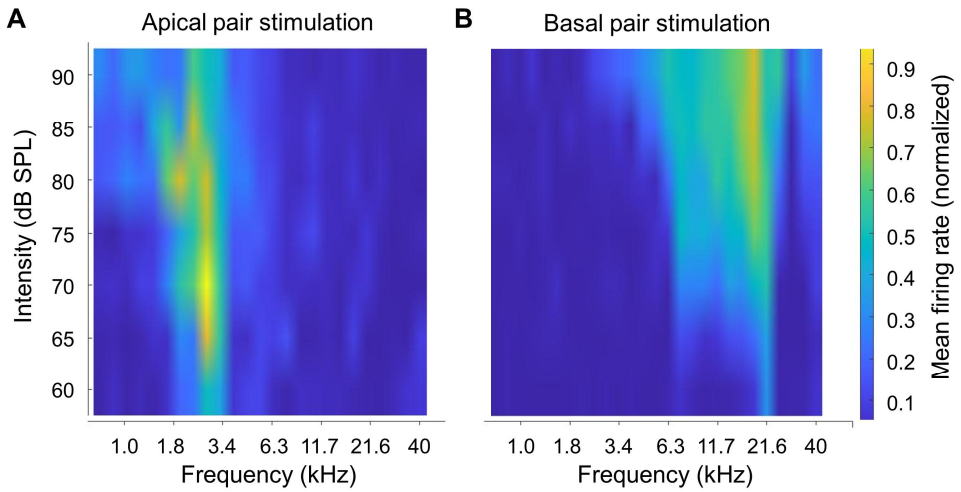

Figure 6. Distribution of the characteristic frequencies in the recording sites that electrically stimulated by apical (A) and basal (B) electrode pairs. Cumulative frequency response area generated by averaging all the firing rates normalized to the maximum of each individual neuron.

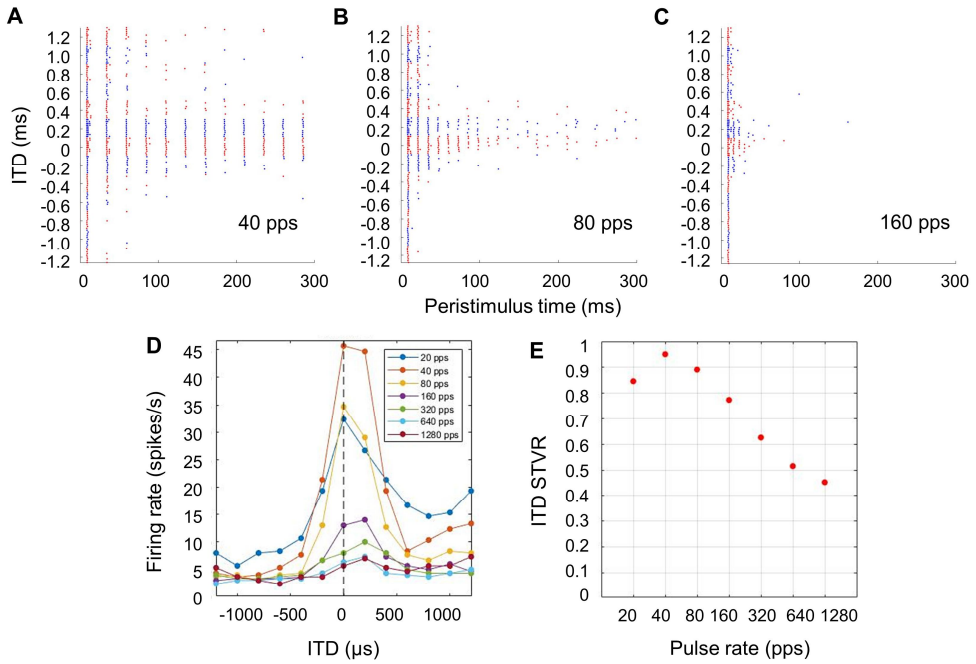

Figure 7. Neural responses of an example neuron with interaural time difference (ITD) sensitivity. (A–C) Temporal spike raster plots to 300 ms pulse trains of three different pulse rates. In each panel, the pulse rate denoted in pulses per second (pps) is shown at the bottom. Alternating colors indicate blocks of stimulus trials at different ITDs. (D) Firing rate versus ITD curves for all pulse rates tested. (E) ITD signal–to–total variance ratio (STVR) as a function of pulse rate. Filled circles indicate statistically significance ($P < 0.01$).

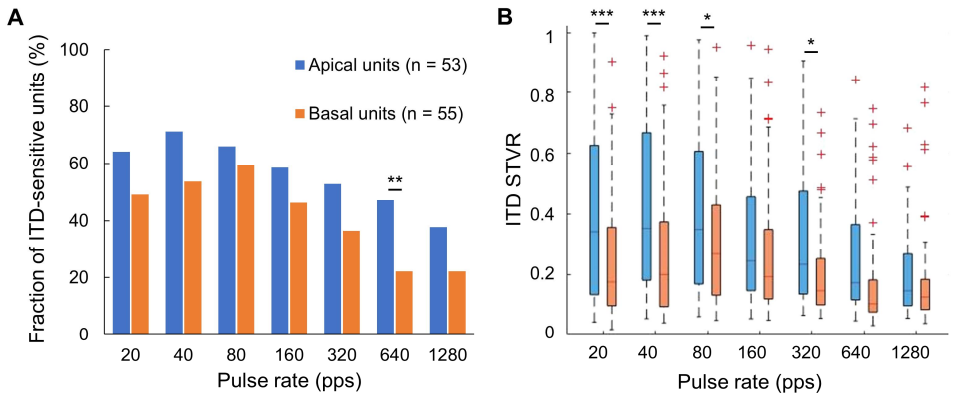

Figure 8. Effects of pulse rate on neural interaural time difference (ITD) sensitivity to apical and basal stimulations. Fraction of neurons with ITD sensitivity (A) and box plots of ITD signal-to-total variance ratio (STVR) (B) as a function of pulse rate for apical and basal units. Fraction of neurons with ITD sensitivity was based on units with STVR at the $P < 0.01$ level. The central line indicates the median, and the bottom and top edges of the box indicate the 25th and 75th percentiles, respectively. The whiskers extend to the most extreme data points within 1.5 times the interquartile range. Significant Bonferroni-adjusted P-values are annotated at the 5%*, 1%**, 0.1%*** confidence level.

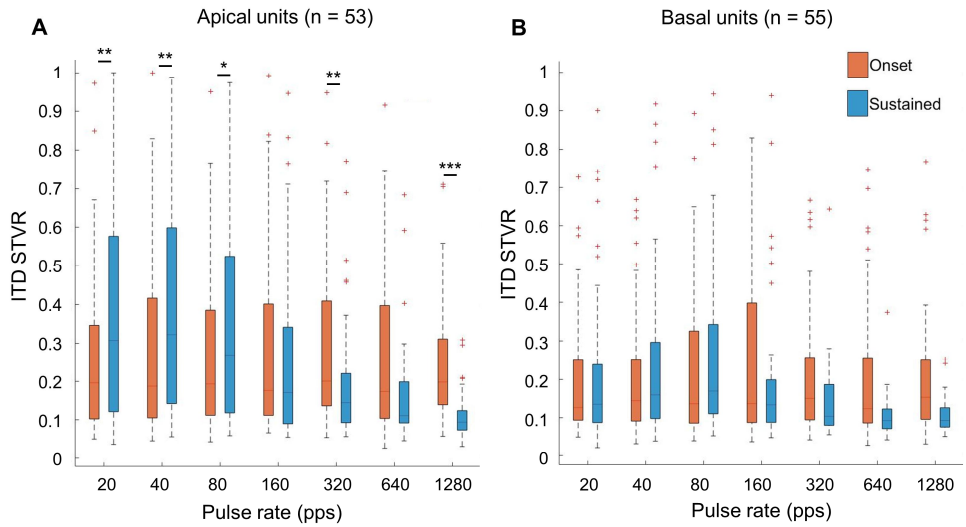

Figure 9. Contribution of onset and sustained responses at different pulse rates on neural interaural time difference (ITD) sensitivity. Box plots of ITD signal–to–total variance ratio (STVR) based on time segments, including onset (0–20 ms) and sustained (20–300 ms), as a function of pulse rate for apical (A) and basal units (B). The central line indicates the median, and the bottom and top edges of the box indicate the 25th and 75th percentiles, respectively. The whiskers extend to the most extreme data points within 1.5 times the interquartile range. Annotated are differences between onset and sustained responses evaluated using a three–way ANOVA test with linear mixed models, and multiple comparisons corrected with a Bonferroni method. Significant Bonferroni–adjusted *P*–values are annotated at the 5%*, 1%**, 0.1%*** confidence level.

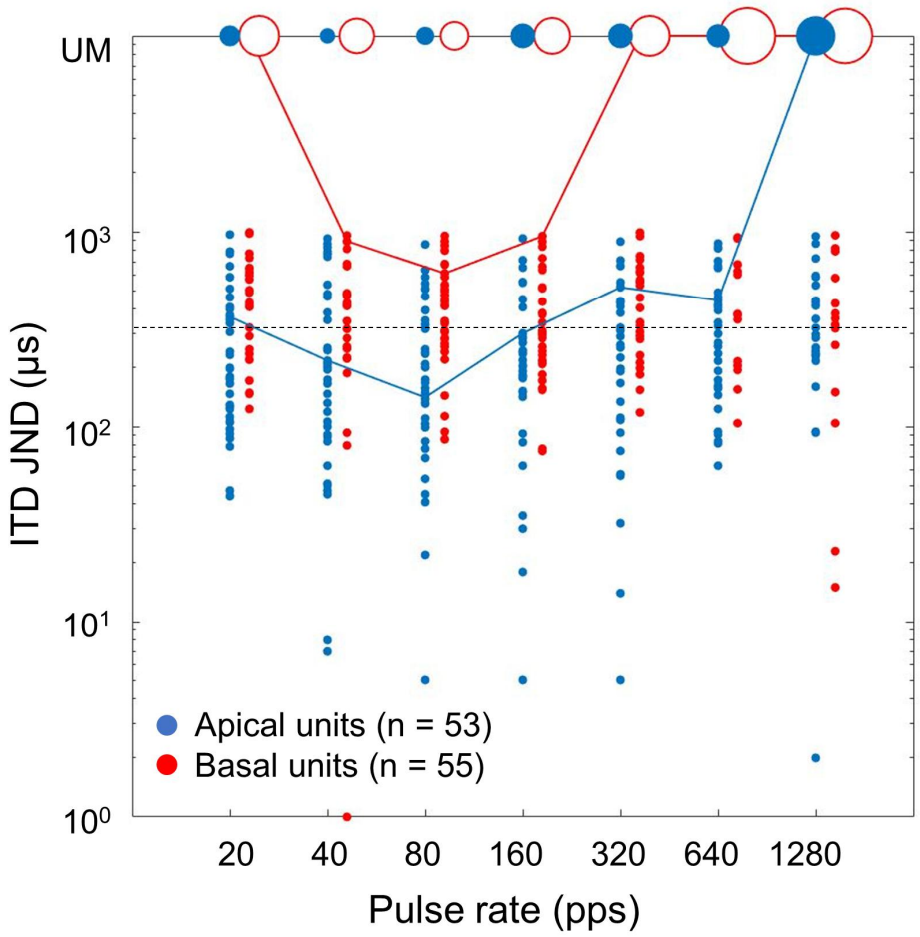

Figure 10. Neural interaural time difference (ITD) discrimination thresholds (just noticeable difference [JNDs]) as a function of pulse rate from individual neurons in the inferior colliculus for apical and basal stimulations. Solid lines represent the median. The area of the circles at the top is proportional to the number of unmeasurable (UM) JNDs. The horizontal black dashed line represents 320 μs (the naturally possible maximum ITD difference in adult rats)

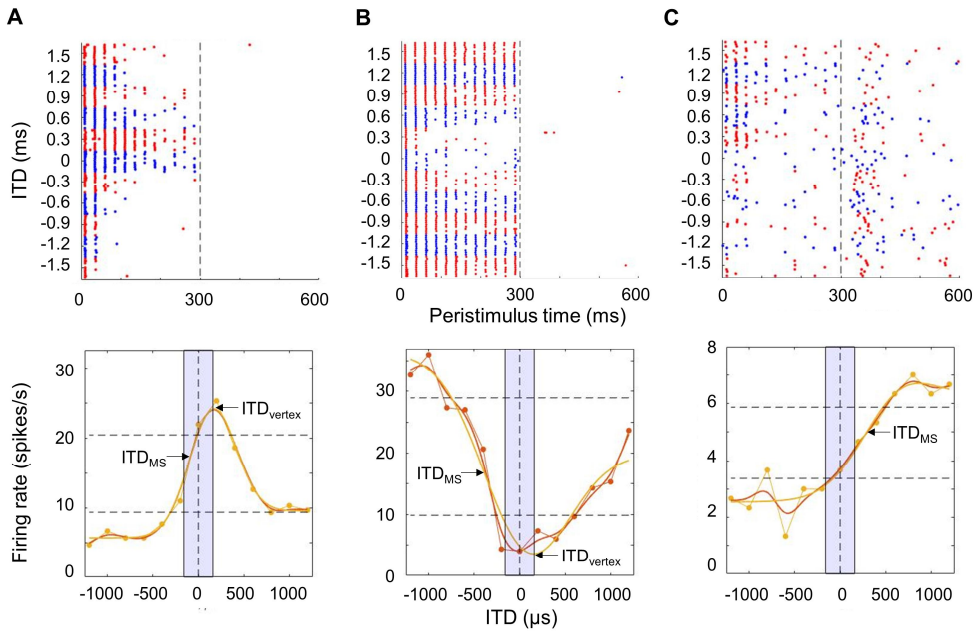

Figure 11. Typical interaural time difference (ITD)-response patterns of three representative units (top) in the inferior colliculus and corresponding ITD tuning types by curve fitting to the data (bottom). Horizontal dotted lines represent the middle 60% of the dynamic range from its minimum response to maximum response, and the gray box illustrates the physiological ITD range of the rat (±160 μs). (A) Peak-type neuron shows a distinct maximum response at ITD_{vertex}, with spike rates decreasing > 20% of the dynamic range at both more negative and positive ITDs relative to the peak. (B) Trough-type neuron shows the opposite pattern with a distinct minimum response at ITD_{vertex}, but with responses increasing >20% of its dynamic range on both sides of ITDs relative to the trough. (C) Monotonic-type neuron whose firing rates

peaked and declined >20% of its dynamic range only for one side of ITDs relative to the peak. The maximum slope position of the ITD tuning curve (ITD_{MS}) is near the midline in the peak-type neuron and away from the midline and outside the physiological range in trough- and monotonic-type neurons.

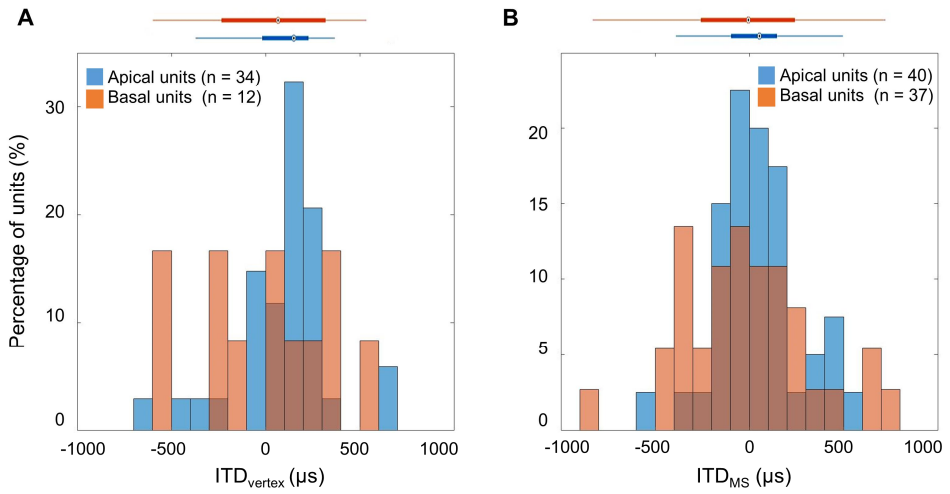

Figure 12. Quantitative characteristics of interaural time difference (ITD) sensitivity. Distributions of ITD_{vertex} (A) and ITD_{MS} (B) for both apical and basal units. Box plots above each histogram represent the median and the 75th and 25th percentiles of the data.

요약(국문초록)

일측 인공와우이식 수술이 양측 고심도 이상의 청각장애 환자에게서 성공적인 청각재활 방법으로 자리잡았으나, 소음환경에서 제한된 효과를 보이는 경우가 많이 보고되었다. 양측 인공와우이식 수술을 시행한 경우 일측 인공와우에 비해 개선된 효과를 보이기는 하나, 양측 인공와우를 통한 양이청취 효과는 정상 청력 청취자에 비하면 현저하게 떨어지는 것으로 보고된다. 이는 주로 인공와우 청취자에게 양이 시간차 감지 같은 소리의 시간적 정보가 제한적으로 전달되기 때문인 것으로 여겨진다.

본 연구는 양측 인공와우의 한계점을 극복하고자 백서의 청각 중뇌인 하구 신경세포에서 전기적 펄스 열의 양이 시간차 감도를 측정하는 신경생리학적 실험을 진행하였다. 와우 내 위치한 양극성 전극쌍을 사용하여 상업적인 인공와우 장치보다 더욱 선택적인 전기자극 방식을 활용하였으며, 와우 내 전기자극의 위치 별로 주파수 특이적인 청신경 자극이 가능하게 하였다. 이를 통해 청각 중뇌의 신경세포의 양이 시간차 감도가 와우내 전기자극의 위치에 따라서 어떻게 반응하는지를 연구하였다. 세포외 단일 신경반응 측정 방법을 사용하여 하구 신경세포의 반응을 기록하였으며, 잘 분리된 신경세포는 와우 첨부 쌍극의 자극 또는 와우 기저부 쌍극의 자극 중 하나에만 반응을 보였다. 저주파를 담당하는 와우 첨부의 전기 자극에 반응하는 신경세포들은 첨부 세포 그룹으로 분류하였고, 고주파를 담당하는 와우 기저부의 전기 자극에 반응하는 신경세포들은 기저부 세포 그룹으로 분류하여 반응을 분석하였다.

와우 내 전기자극의 위치에 무관하게 첨부 세포 그룹과 기저부 세포 그룹 모두에서 70%이상의 신경세포들이 전기적 자극의 양이 시간차에 대한 감도를 보였다. 하지만, 전기 자극 빈도에 대한 신경적 양이 시간차 감도의 의존성은 와우 내 전기자극의 위치별로 유의한 차이를 보였다. 또한, 양이 시간차 감지 역치와 양이 시간차 조율 곡선의 형태별 발생 빈도도 첨부 세포 그룹과 기저부 세포 그룹에서 유의한 차이를 보였다. 와우 첨부에 전기적인 자극을 주는 경우, 기저부 자극에 비하여 봉우리 형의 양이 시간차 조율 곡선의 높은 발생 빈도를 보였으며, 대부분의 봉우리 형의 곡선에서는 가장 가파른 곡선 기울기를

보이는 위치가 백서의 생리적인 양이 시간차 감지 범위인 ±160 μs 내에 위치하였다. 그 결과, 첨부 세포 그룹에서 기저부 세포 그룹에 비해 보다 좋은 양이 시간차 감지 역치를 갖는 것으로 나타났다.

본 연구의 결과들은 청각 중뇌인 하구에서 이루어지는 양이 시간차에 대한 처리 과정이 와우로부터 연결되는 주파수 특이 청각로별로 분리되어 있다는 평행 처리 경로 이론을 뒷받침하고 있으며, 임상적으로도 양측 인공와우의 시간적 양이 효과 개선을 위해서는 저주파수 특이 경로를 보다 선택적으로 자극하는 것이 중요하다는 점을 제시하고 있다.

주요어 : 인공 와우, 양이 효과, 양이 시간차, 청각 중뇌, 하구
학 번 : 2019-34393